Revista Internacional de
Ingeniería
de Estructuras

Vol. **20,2**, 135 - 157 (2015)

STATE OF THE ART IN STABILITY OF RC STRUCTURAL WALLS

Ana Gabriela Haro
Departamento de Ciencias de la Tierra y la Construcción
Universidad de Fuerzas Amadas ESPE
Av. Gral. Rumiñahui s/n, Sangolquí.

Department of Civil, Construction, and Environmental Engineering
North Carolina State University
Raleigh, NC 27695

Correo Electrónico: agharo@ncsu.edu

ABSTRACT

Reinforced concrete structural walls are utilized in seismic design of multistory buildings as systems that exhibit high levels of strength and ductility under ultimate loads. In the recent 2010 Chile and 2011 New Zealand earthquakes, a failure mode related to inelastic lateral instability, which had been observed only in laboratory tests, generated significant damage to buildings that included rectangular or flanged wall geometries. This paper focuses on the state-of-the-art research in local buckling behavior of structural walls. Experimental programs for planar walls where this mechanism was captured are described. Key findings to take into account to prevent inelastic lateral instability in structural walls are additionally presented.

Keywords: structural walls, inelastic lateral instability, out-of-plane local buckling

1 INTRODUCTION

Reinforced concrete structural walls (RCSWs) are used as effective lateral resisting systems in countries located in regions susceptible to severe earthquakes or wind loads. In fact, the inclusion of ductile RCSWs in multistory buildings improves their seismic performance considerably. Widespread experimentation programs involving different geometries and material properties have been developed all around the world resulting in improved design and construction processes. The most common types of wall sections utilized are rectangular, flanged and barbell. Generally, the preferences depend on the building configurations; however, in recent years thinner walls have become more prevalent due to growing engineering costs and higher compressive strengths for concrete (Wallace, 2012).

Since poor structural performance has been observed in recent earthquakes, more reliable procedures are required to identify the non-linear behavior of RCSWs to avoid not only loss of life but also damage to property.

Recibido: Febrero de 2015
Aceptado: Julio de 2015

There is still a gap between actual failure modes produced in the boundary elements of thin RCSWs and simulations through numerical models. This fact has been recognized from reported damage after the occurrence of strong motions during the 2010 Chile and 2011 New Zealand earthquakes. In addition to concrete crushing and reinforcement rupture failures, out-of-plane local buckling remains as an unsolved problem (Sritharan, et al., 2014).

Figure 1 shows the RCSW of a seven-storey office building that experienced local buckling during the 2011 New Zealand earthquake. The failure was attributed to flexural tension yielding followed by instability of the plastic hinge region (Kam, Pampanin, & Elwood, 2011).

Figure 1 Local buckling damage of a RCSW in a seven-storey building during the 2011 New Zealand Earthquake. (Kam, Pampanin, & Elwood, 2011)

Goodsir (1985) first studied this failure mechanism in a research program conducted to propose a capacity-based seismic design methodology. It was defined as the effect of large inelastic tensile strains accompanied by cracking of the boundary elements at the level of the plastic hinge region. Under load reversals, out-of-plane deformations can be generated in the compression zone as a consequence of two possible scenarios: remaining horizontal open cracks, and exceedance of limit tensile strains. Later Paulay and Priestley (1993) developed a model to characterize the relationship between in-plane tensile strains and out-of-plane wall displacement resulting in instability. Local buckling damage of a RCSW is depicted in Figure 2.

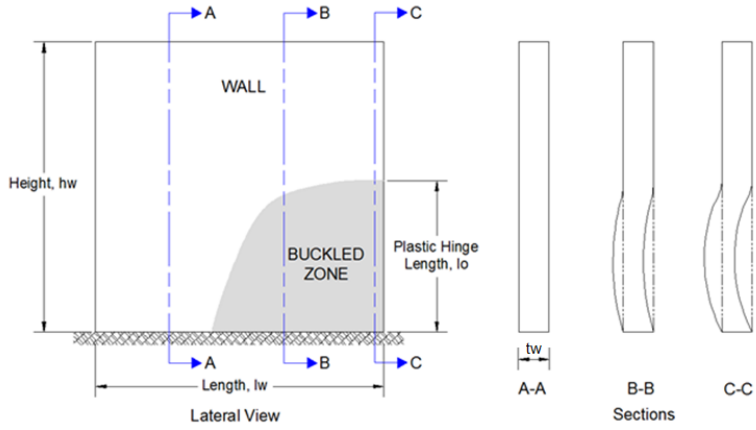

Figure 2 Local buckling damage representation of RCSW

In the following sections observed wall buckling damage in the 2010 Chile and 2011 New Zealand earthquakes is described. In addition, laboratory studies for thin RCSWs where out-of-plane buckling was captured are also analyzed. And finally, the state-of-the-art buckling mechanism of structural walls is detailed.

2 INELASTIC LATERAL INSTABILITY OBSERVED IN RECENT EARTHQUAKES

Structural wall systems and dual systems, the latter known as wall-frame structures (Paulay & Priestley, 1992), have been utilized since the 1960s for medium to high-rise buildings located in urban areas (Moroni, 2002). Reports originated after important seismic events have provided valuable information about the performance of RCSWs buildings. Table 1 shows the details of selected historical earthquakes and the number of damaged RCSWs buildings affected during each event.

Table 1 Historical earthquakes where damage in RCSWs was reported

Earthquake	Date	M	PHGA (g)	Depth [km]	# of RCSWs Buildings
Alaska (USA), 1964	03-27-1964	9.2	0.14-0.18	25	10
San Fernando (USA), 1971	02-09-1971	6.6	0.30 ; 1.25*	8.4	7
Vrancea (Romania), 1977	03-04-1977	7.5	0.16-0.20	94	100
Chile, 1985	03-03-1985	7.8	0.67	33	3
Mexico, 1985	09-19-1985	8.1	0.22	18	4
Loma Prieta (USA), 1989	10-17-1989	6.9	0.64	18	3
Northridge (USA), 1994	01-17-1994	6.8	1.0 ; 1.82*	18.5	6
Kobe (Japan), 1995	01-17-1995	6.9	0.50-0.80	22	12
Kocaeli (Turkey), 1999	08-17-1999	7.4	0.41	15.9	10
Chi Chi (Taiwan) 1999	09-21-1999	7.3	1.1	8	1
Maule (Chile), 2010	02-27-2010	8.8	0.65	35	14
Christchurch (New Zealand), 2011	02-22-2011	6.3	0.7; 1.6*	5	47

* First value corresponds to the peak horizontal ground acceleration PHGA recorded in populated areas and the second value constitutes an exceptional case.

Historically, diagonal cracking, web crushing, compressive boundary element damage, horizontal failure plane and collapse have been the dominant type of damage identified for the buildings where partial or full replacement of a wall was required (Birely, 2011). However, local buckling instability was noticed only in the 2010 Chile and 2011 Christchurch earthquakes.

On February 27, 2010 an 8.8 magnitude earthquake struck Chilean regions for about three minutes producing substantial losses. The maximum recorded peak ground acceleration was 0.65g. Mid- to high-rise RC buildings in Santiago depicted failure of their structural walls in the lower storeys. Figure 3(a) shows the overall view of a 18-storey building that suffered from the local buckling failure mode. Figure 3(b) demonstrates the damage in one of the slender walls located at the parking level. It was the first time where out-of-plane instability phenomenon was captured in a real structure. The average thickness of the walls was 200mm and the height-to-width ratio was close to 18, maximum value recommended by the Chile concrete design standard (NCh 433 1996) (Saatcioglu et al., 2013). The failure was attributed to the slenderness of boundary zones prone to buckle under compression loadings.

(a) (b)

Figure 3 RC 18-storey building in Santiago: (a) Overall view of the building; (b) wall local buckling failure (Wallace & Moehle, 2012)

In February 22, 2011 New Zealand registered a 6.3 magnitude earthquake where Christchurch was severely damaged since the hypocenter was located below the city. Peak accelerations of 2.2g and 1.7g were recorded in the vertical and horizontal directions, respectively. The Christchurch earthquake was preceded

by the Mw 7.1, Darfield earthquake on September 4, 2010. For many seismologists it is considered an aftershock.

Figure 4(a) and (b) shows the overall view and the structural performance a wall in the Pacific Brands House (PBH), respectively. The PBH was a 7-storey RC building constructed in 1984 which included 2 L-shaped walls of about 300 mm thick. The boundary element of the north wall in the lower level developed an out-of-plane buckling failure, which was accompanied by significant concrete damage on its surrounding areas. The cyclic combinations of compression strains preceded by large tension strains were assumed to be the cause of this phenomenon (Sritharan, et al., 2014). Contrary to what was exposed for the 2010 Chile Earthquake, the PBH building included thicker RC walls but a lower ratio of these structural elements against the total plan area.

(a) (b)

Figure 4 RC 7-storey building in Christchurch: (a) Overall view of the building; (b) wall local buckling failure (Sritharan, 2011)

3 STRUCTURAL PERFORMANCE OF RCSWs IN LABORATORY TESTS

A significant number of experimental programs have been performed to examine the behavior of RCSWs for different geometries and mechanical properties. Nevertheless, considering the fact that the aim of this analysis is to assess the local buckling failure mode, the tests of walls where the mentioned phenomenon was observed or studied is first presented in this section, followed by the results of tests carried on prisms replicated as boundary elements of planar RCSW.

3.1 Laboratory studies in planar walls

Table 2 summarizes the parametric study of tests carried on thin RC walls, where out-of-plane buckling was captured. In this table, t_w, h_w and l_w are the thickness, the total height and the length of the RC walls, respectively; ρ_b is the longitudinal reinforcement ratio of the boundaries elements; ρ_h is the transverse reinforcement ratio of the wall web; and ρ_l is the distributed longitudinal web reinforcement ratio. The detailed reinforcement corresponds to the web regions but not to the flange zones of the T-shaped sections which include the letter T in the name of the specimen.

Table 2 Parametric Study – Experimental programs that reported local buckling in RC Walls

Test Name	Walls	Material Properties		Geometry			Reinforcement			ALR Or AAL** [kN]	Lateral Load Pattern
							boundary	web			
		f'c [MPa]	fy [MPa]	t_w [mm]	l_w [mm]	h_w [mm]	ρb [%]	ρl [%]	ρh [%]		
Vallenas et al. (1979)	**R1***	27.5	482	114	2412	3.085	5.57	0.54	0.54	0	monotonic
	R2*										cyclic
Oesterle et al. (1976)	F1	38.2	442	102	1905	4570	3.89	0.30	0.71	0	cyclic
	F2	45.3	428				4.35	0.31	0.63	1256	cyclic
	R1	44.5	509				1.47	0.25	0.31	0	cyclic
	R2*	46.2	448				4.00	0.25	0.31	0	cyclic
Goodsir & Paulay (1985)	**R1***	28.6	450	100	1500	2400	4.71	0.94	0.71	0.263	cyclic
	R2*	25.3	450		1500		4.71	0.94		0.163	cyclic
	T3*	33.8	400		1300		3.93	0.76		0.118	cyclic
	R4*	36.5	345		1500		4.71	0.94		0.153	cyclic
Thiel et al. (2000)	**WPH2***	30.0	470	100	1000	4000	3.5	0.4	0.42	0.15	cyclic
	WPH3						3.5	0.4	0.42	0.04	cyclic
	WPH4*						1.6	0.4	0.42	0.15	cyclic
Thomsen & Wallace (2004)	RW1	27.4	414	102	1219	3658	2.93	0.33	0.46-0.49	0.1	cyclic
	RW2						2.93	0.33	0.69-0.37	0.07	cyclic
	TW1						2.93	0.33	0.46-0.49	0.09	cyclic
	TW2*						0.70	0.44	0.92-0.53	0.075	cyclic
Brueggen (2009)	NTW1	50.1	414	152	2286	7315	3.78	0.59	0.26	829.59	cyclic
	NTW2*	45.3				3658	2.16	2.16	0.41		cyclic
Aaleti et al. (2012)	**RWN***	34.5	414	150	2280	6400	3.8-9.0	0.37	0.68-0.85	0	cyclic
	RWC*										cyclic
	RWS										cyclic
Alarcón (2013)	**M1***	27.4	420	100	700	1600	0.45	0.72	0.44	0.15	cyclic
	M2*									0.25	cyclic
	M3*									0.35	cyclic
Marihuén (2014)	**M4***	27.4	420	75	700	1600	0.49	0.67	0.46	0.15	cyclic
	M5*			100		1180	0.45	0.72	0.44		cyclic
	M6*			100		1600	0.0	1.34	0.44		cyclic
	M7*			100		1600	0.45	0.72	0.44		cyclic
	M8			100		1600	0.45	0.72	0.64		cyclic
	M9*			100		1600	0.45	0.72	0.56		cyclic

* Buckled specimen; ** ALR – Axial Load Ratio, AAL – Applied Axial Load

Description of the laboratory studies in planar walls

In order to accomplish a better understanding of the behavior of RCSW subjected to high shear seismic loading, Vallenas et al. (1979) experimented eight earthquake tests on three-storey 1:3 scaled RC walls from prototypes of ten- and seven-storey buildings designed in accordance to in progress code requirements.

This research involved the study of the influence of parameters like: type of confinement in the boundary elements, wall cross-section, moment-to-shear ratios, monotonic and cyclic load patterns, and repair procedures. Two barbell walls and two rectangular walls were considered in the study. After subjecting the specimens to the established loading conditions, they were repaired and tested again. Steel tensile strains reached in the boundary elements and the corresponding crack widths and spacing were identified as determining parameters to cause local buckling under load reversals (Vallenas, Bertero, & Popov, 1979).

A total of two rectangular walls, ten barbell walls, and two flanged walls were tested under monotonic and incrementally increasing reversed loading (Oesterle, Fiorato, Aristizabal-Ochoa, & Corley, 1979). Two of the barbell walls were repaired and tested once more. The objectives of the study were to determine ductility levels, load-deformation characteristics, energy dissipation capacity and strength of the walls. Wall R2 was the only one that reported out-of-plane buckling of the compression zone. It was caused by "alternate tensile yielding" of the flexural reinforcement in the boundary elements (Oesterle et al., 1976). The load-carrying capacity of the wall was reduced by the large out-of-plane deformation developed in the lower 910 mm (3ft) after several load reversals. Rebar buckling and fracture were captured for the remaining three walls.

With the intention of studying the mechanism of out-of-plane instability and the existing code provisions for confinement in critical sections subjected to large compression strains, Goodsir and Paulay (1985) applied cyclic lateral loads in combination with different axial load ratios (ALR) to a set of three rectangular walls and one T-section wall. The four specimens exhibited out-of-plane buckling in the boundary elements. The slenderness of the specimens was considered the reason to provoke this behavior. The failure modes detected for walls R1 and R4 suggested material failure instead of lateral instability. The full east end of the wall R2 buckled before returning to the original vertical position during the last cycles. The web of the wall T3 experienced lateral instability, and during consecutive reversals the flange failed in compression.

Three 1:3 scaled rectangular walls were tested by Thiel et al. (2000) where extreme pseudo-dynamic loads were applied. The influence of the reinforcement content and the axial force were investigated. The results reported local buckling for walls WPH2 and WPH4 at 400% and 300% of an artificially generated earthquake, respectively. Wall WPH3 did not present out-of-plane buckling behavior. The most significant conclusions from the tests were (Thiel, Wenk, & Bachmann, 2000)(p. 84): the influence of reinforcement ratio and axial force on the behavior of RC structural walls under earthquake action must not be neglected; under low and moderate earthquakes, a high axial force is advantageous: the plastic deformation and the axial elongation of the wall at the end of the earthquake are reduced, the stiffness at small deformation increases; and, under strong earthquakes, the low energy dissipation of walls with high axial force becomes relevant. Consequently, walls with high axial force will fail prematurely.

Six quarter-scale wall specimens were tested under the experimental verification carried out by Thomsen and Wallace (2004), but only the results for the

two solid rectangular (RW1, RW2) and two T-shaped (TW1, TW2) walls cross sections are incorporated in this analysis. The four specimens were subjected to cyclic lateral displacements in combination with axial loads of approximately $0.10A_g f'_c$. Specimen RW1 reported significant loss in lateral load capacity when buckling of the longitudinal reinforcement was produced at 2.5% drift. RW2 behaved similarly but because of the closer spacing of the hoops at the boundary elements, the lateral load capacity was maintained longer. Specimen TW1 experienced brittle failure for a drift of 1.25% where buckling of the bars located along the boundary element and the web was observed. Even though the lateral load capacity for the specimen TW2 exceeded the response from TW1, it was affected by out-of-plane buckling caused by a very narrow confined core.

Two T-shaped RCSWs were subjected to multidirectional cyclic loading as part of a research program focused on developing a simplified modeling approach to predict the response of structural walls under the philosophy of performance-based design (Brueggen, 2009). For the NTW1 wall, the failure in the flange-in-tension direction was caused by the failure of the confinement in the boundary element of the web; consequently, the concrete core crushed and the longitudinal reinforcing buckled. This behavior was associated with unwinding of the confining hoops close to the base of the web tip. Based on the structural performance of the NTW1 wall, when constructing the NTW2 wall, the open corner of the hoops was relocated out of the extreme compression reinforcement and additionally the confined region was extended. The modifications led to a failure caused by fracture of the confining reinforcement. Moreover, it was concluded that increasing the length of the boundary elements produced an irrelevant effect on the general structural behavior of the latter specimen whose north flange experienced out-of-plane buckling. The results also demonstrated that the skew-direction loading did not increment significantly the maximum compression strains in comparison to the orthogonal loading at the same drift level.

To investigate the consequences of considering continuous reinforcement (N), lap splices (S), and mechanical couplers (C) in the plastic hinge region, three identical rectangular RCSWs were built and subjected to cyclic reversal loadings by Aaleti et al. (2013). Two different boundary elements were included in the design with the purpose of accounting for a flange. Specimens RWN and RWC experienced lateral instability in the left boundary elements by the time a 2% drift was reached. The reason for this behavior was attributed to the combination of large compressive forces, large tensile strains developed in previous cycles, large in-plane displacements, and the lack of out-of-plane supports at the level of the floor diaphragms (Aaleti et al., 2013). Specimen RWS with twice the longitudinal reinforcement of the buckled walls did not reflect lateral instability.

After the 2010 Chile earthquake some experimental programs have been conducted in that region in order to reproduce the different observed failure modes in RCSWs. In particular, Alarcón (2013) tried to capture the influence of the axial load ratio (ALR) in the seismic structural performance of thin walls without seismic detailing. A prototype was established in function of a survey of walls damaged in the mentioned earthquake. This project involved the construction of three 1:2 scale identical RC wall specimens subjected to in-plane double-cycle increasing

displacements following the application of axial loads. Constant ALRs of 0.15, 0.25, and 0.35 were considered for each specimen. The failure mode detected in the three walls was controlled by axial-flexure interaction associated with a relatively high M/Vl_w ratio of 2.5, where M and V are the moment and shear at the cross section under consideration, respectively. The sequence of the observed structural behavior for the three walls was: flexural cracking, reinforcement yielding, vertical cracking, concrete spalling and reinforcement buckling accompanied by opening of horizontal reinforcement, concrete crushing failure, and wall buckling. Out-of-plane buckling was developed as a consequence of compressive failure and low wall thickness. The results indicated that high ALRs induce substantial decrease in the ultimate curvature, displacement capacity, and ductility (Alarcón, 2013).

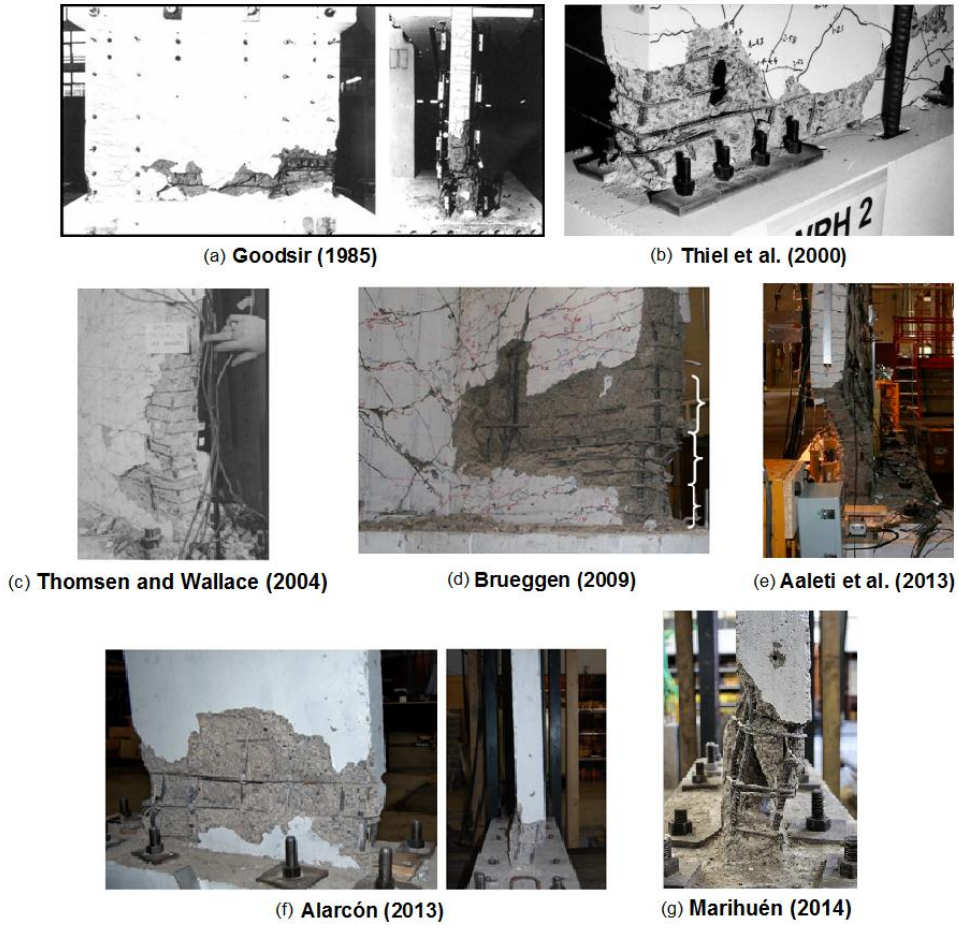

Figure 5 Final state of tested walls

Marihuén (2014) tested 6 walls in total. This research was part of the big experimental program where Alarcón (2013) was involved. A wall length *lw* of 700 mm was considered for all cases. In general, five specimens suffered out-of-plane

buckling after crushing was produced at the base of the walls. Only wall M8 behaved differently. It failed in flexural compression without exhibiting local buckling after crushing. The difference can be attributed to the transverse reinforcement distribution, which consisted in locating the confinement along the space between the principal horizontal reinforcement (Marihuén, 2014).

Figure 5 shows the final state of some of the walls presented in this section.

3.2 Laboratory studies in prisms

Noticing the concentration of damage in the boundary elements of thin RCSWs due to higher stress and strain demands, some investigations have been carried on prisms, which was found as an economical way to study the inelastic instability of RCSWs. In general, the main objective of these tests focuses on subjecting specimens to cyclic tension and compression actions to simulate vertical components of actual seismic loading. Table 3 summarizes the principal parameters that varied in the studies reviewed in this section.

Table 3 Parametric Study - Prisms

Test Name	# of tested prisms	Material Properties		Geometry			Reinforcement		Tensile Strains [%]	Axial Load Type T-Tension C-Comp.
		f'c [MPa]	fy [MPa]	Cross Section [mm^2]	Cover [mm]	Height [mm]	Lon. [%]	Tran. [mm]		
Goodsir (1985)	9	24.1 29	442	160x480	17.5 18.5	1120 880 640	3.1	64 96	2.35 2.425 2.5	axial reversed cyclic T - C
Chai & Elayer (1999)	14	34.1	375 455	102x203	12.5	1199 1505 1811	2.1 3.8	57 76	1.0	axial reversed cyclic T - C
Creagh (2010)	2	30	460	152x305	19	915	3.7	50.8	3.6	T - C C
Chrysanidis & Tegos - I (2012)	5	24.89	604	75x150	8	760	2.68	33	0.0-5.0	1 cycle T - C
Chrysanidis & Tegos - II (2012)	11	22.22-23.33	604	75x150	8	760	1.79- 10.72	33	3.0	1 cycle T - C
Shea & Flintrop (2013)	8	28	414	152x381	34.9	762	2.9	114.3 152.4 203.2	4.5 3.0 2.0	axial reversed cyclic T - C

Description of the laboratory studies in prisms

The tests completed by Goodsir (1985) consisted on nine prisms as part of the experimental program conducted on four cantilever structural wall units, described previously. Once concluded the tests on the RCSWs, it was observed the potential for out-of-plane instability developed in the boundary elements when the walls were subjected to reversing lateral loads. Aspect ratios of 7, 5.5, and 4 were utilized. Axial deformations were imposed to reach the set strains in tension and compression. Only unit #3 was imposed a monotonic load and it performed well. The specimens with the two highest aspect ratios developed buckling failure.

The two units with aspect ratio of 4 reported a failure associated with concrete crushing although out-of-plane deformations were recorded. Degradation of bond between the longitudinal reinforcement and the concrete was identified to be more critical at higher strains for cyclic loading in comparison to monotonic loading. An unsuccessful attempt to predict the out-of-plane displacements of the prisms was developed in this research based on Euler buckling theory. It was the first time that local buckling mechanism of RCSWs was established as a function of the tensile strain levels reached in the boundary zones. It is highlighted the fact that buckling instability is prone to happen with increasing aspect ratios and high tensile strain levels (Paulay & Goodsir, 1985).

Once recognized that the tensile strains imposed on a RCSW is a critical parameter that governs its lateral stability, Chai and Elayer (1999) tested fourteen prisms in order to establish the maximum tensile strain that a ductile prism could sustain under quasi-static axial forces. The axial reversed cyclic loading comprised an initial half-cycle of axial tensile strain followed by a compression half cycle. The target compressive strain for twelve prisms consisted on 1/7 of the axial tensile strain and for the other two specimens it was 1/5. Chai and Elayer (1999) (CEBM) proposed a phenomenological model based on a kinematic relation between the axial strain and the out-of-plane displacement that had been developed previously by Paulay and Priestley (1993) (PPBM) in function of what had been recommended earlier by Goodsir (1985). When the maximum tensile strain values predicted from the CEBM and PPBM formulations were compared with the tests results, both methods showed to be conservative. However, the CEBM resulted to be more accurate (Chai & Elayer, 1999).

Two prisms were tested by Creagh et al. (2010) to demonstrate how the tensile strains reached in boundary elements affect the load bearing capacity and incite a buckling failure mode. The first prism was tensioned until yielding and then it was subjected to tensile strains of 1.5, 2.0, 3.0, and 4.0% followed by a compressive action until failure. The second prism was only exposed to compression. It was noticed that the specimens reported two different failure modes. Prism #1 evidenced buckling instability and prism #2 suffered a brittle failure due to concrete crushing in the upper zone.

In order to study the effect of high tension strain levels reached in boundary edges of thin RCSW with respect to the ultimate bearing capacity as a function of a decrease in the effective rigidity, five identical specimens 1:3 scaled were tested by Chrysanidis & Tegos (2012). The specimens were subjected to five degrees of elongation with values of 0.0, 1.0, 2.0, 3.0, and 5.0%, respectively. A uniaxial tensile load followed by a compression load constituted the loading pattern for the experiments. Different structural behaviors were detected in the process. The last two specimens with degrees of elongation 3.0% and 5.0% experienced a significant resistance decrease in the order of 38% and 26%, respectively. The failure mechanism recounted for these specimens was related to global buckling. The three first specimens reported different failure modes related to crushing of the compression zone. This study identified the lateral instability as a complex phenomenon that requires further examination because it does not only depend on aspect ratios as suggested by some design codes (Chrysanidis & Tegos, 2012).

With the aim of completing the previous investigation, another eleven specimens with similar geometry but different longitudinal reinforcement ratios, between 1.79% and 10.72%, and different concrete strengths were tested by Chrysanidis & Tegos (2012). All specimens were tested at a single tensile strain degree of 3.0% before exposing them to a compression load to complete the cycle. As a result, two important outcomes were specified: first, an increment in the longitudinal reinforcement ratio does not influence the failure mechanism because out-of-plane buckling was reported for all cases; and second, the mentioned increment does not always lead to a buckling failure load rise but it seems to depend on the rebar distribution.

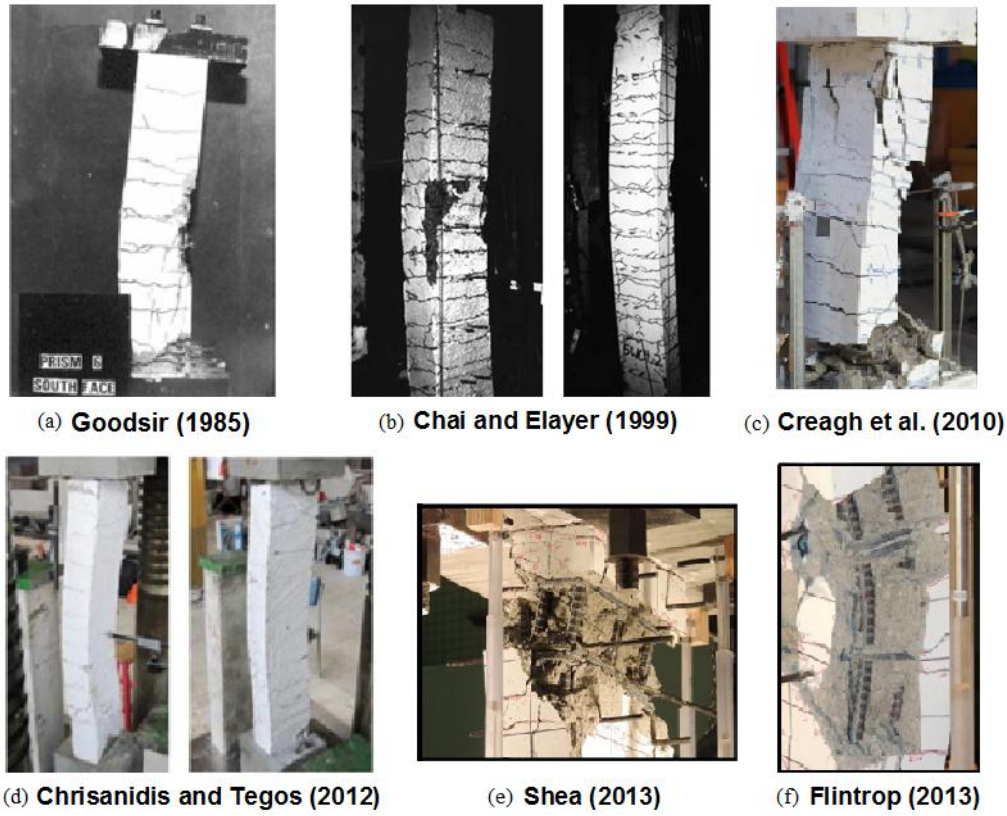

Figure 6 Final state of prisms

Eight reinforced concrete prisms were subjected to cyclic testing as part of the 2013 NEES@UCLA project (Shea, 2013) (Flintrop, 2013). The longitudinal reinforcement and the prism height were conserved identical for all eight specimens but only hoop spacing was varied. The tests consisted on inputs of diverse magnitudes for maximum compression strains of 0.2% to 0.6% and maximum tensile strains of 2.0% to 4.5%. Prisms #1, #2, and #4 evidenced rebar buckling as a failure mode. Prism #3 reported global buckling similar from what

prisms #5 and #6 revealed at the end of the tests (Flintrop, 2013). Prisms #7 and #8 failed due to global buckling and concrete crushing, respectively (Shea, 2013). The conclusions from this project were: first, a limit for the concrete cover should be provided to guarantee the stability in the core; and second, a limit for the wall thickness must be required when large tension and compression strains are expected, which has been considered for various design codes previously.

Figure 6 shows the final state of the prisms depicted in this section.

The results of the experiments carried out for walls and prisms reflect the necessity of supplementary research to assess the local buckling mechanism of ductile RCSWs.

4 STATE OF THE ART IN OUT-OF-PLANE INSTABILITY PREDICTION

4.1 Paulay and Priestley (1985) and Chai and Elayer (1999) models

Goodsir (1985) first described the mechanism of out-of-plane instability, once it was clearly exhibited during his research program as detailed previously. In summary the mechanism consists on different stages developed as follows when walls are subjected to cyclic reversal of in-plane loading. At high displacements in one direction, large tensile strains are developed in one of the boundary elements, along the plastic hinge region, accompanied by wide horizontal cracks. While unloading throughout the opposite direction, compression strains, originated from the axial load and the moment caused by its eccentricity, tend to balance the remaining tensile strains. During this stage as the in-plane lateral load keeps increasing, out-of-plane deformations could develop. The described behavior is presented in Figure 7, which shows the deformations and strain patterns in the plastic hinge region of RCSWs.

Figure 7 illustrates two possible scenarios. First, if the horizontal cracks close before reaching a critical state, explained below, the out-of-plane deformations are small and the compressive force is sustained without exhibiting instability. On the contrary, if the horizontal cracks remain open, large out-of-plane deformations develop and consequently instability is evidenced by a drop in the strength of the wall.

In order to capture the critical stage, Paulay and Priestley (1993) developed a model that includes the relationship between tensile strains reached under in-plane loading and out-of-plane deformations manifested simultaneously under reversal loading; additionally, the model suggests an out-of-plane displacement limit to prevent wall local buckling.

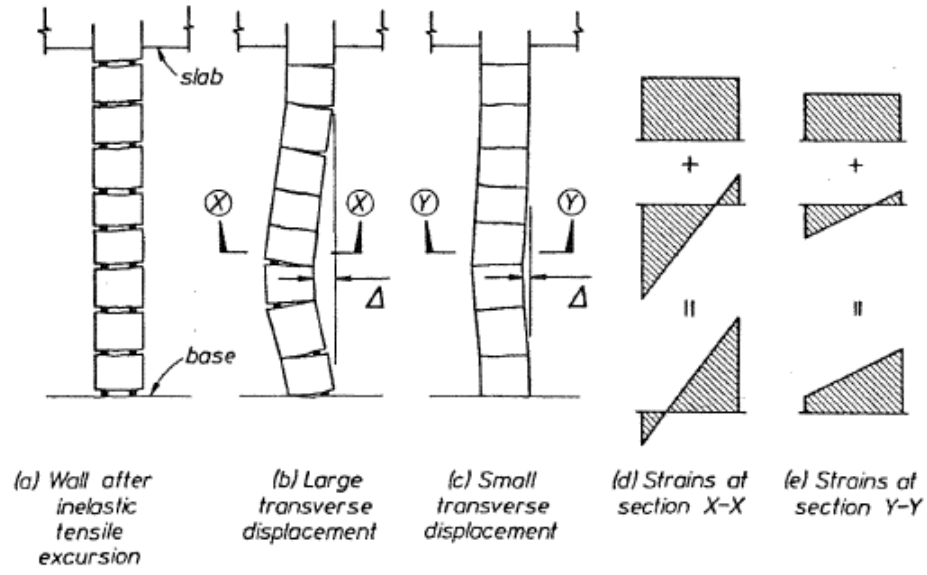

Figure 7 Deformation and strain patterns in a plastic hinge region, Goodsir (1985)

In this context, (1) suggests a maximum tensile strain value to ensure lateral stability of structural walls.

$$\epsilon_{sm} \leq 8\beta \left(\frac{b}{l_o}\right)^2 \xi_c \tag{1}$$

where, $\beta = d/b$ is a parameter defining the position of the longitudinal reinforcement; b and d are the thickness and the transverse effective depth of the wall section, respectively; l_o is the buckled length of the wall, which may be taken equal to the plastic hinge length of the wall, as recommended by Paulay and Priestley (1992). Additionally, a stability criterion ξ_c was established:

$$\xi_c = 0.5\left(1 + 2.35\, m - \sqrt{5.53\, m^2 + 4.70\, m}\right) \leq 0.5 \tag{2}$$

where, m is the mechanical reinforcement ratio:

$$m = \rho_{end} \frac{f_y}{f_c'} \tag{3}$$

here, ρ_{end} is the local longitudinal reinforcement ratio of the end region of the wall, f_y is the yield strength of the longitudinal reinforcement, and f_c' is the uniaxial compressive strength of the concrete.

In accordance with this approach, Chai and Elayer (1999) carried out the described experiment on prisms and proposed a less conservative phenomenological formulation (4) to evaluate axial tensile strains developed in the boundary elements of RCSWs in order to prevent local buckling behavior when exposed to reversal loading.

$$\epsilon_{sm} \leq \frac{\beta}{c}\left(\frac{b}{l_o}\right)^2 \xi_c + 3\,\epsilon_y \quad (4)$$

where, ϵ_y is the yield strain of the longitudinal reinforcement; c is a coefficient that reflects the variation of the curvature along the buckling zone; and, β is the ratio between the position of the extreme layer of reinforcing steel and the thickness of the wall. If the wall has only one longitudinal reinforcement layer, then $\beta = 1/2$.

Chai and Elayer (1999) assumed a sinusoidal curvature distribution $c = 1/\pi^2$. Paulay and Priestley (1993) considered a constant curvature distribution which had been suggested by Goodsir (1985) earlier. Equation (4) additionally includes the effect of strains elastically recovered during initial reloading and strains required to yield the reinforcement in compression, parameters that account for the hysteretic behavior of the longitudinal reinforcement.

The experimental outcomes from Chai and Elayer (1999) study were compared with the maximum tensile strains predicted by the two described models. Equations (1) and (4) resulted to be conservative, but could be included in design procedures to bound the wall thickness of rectangular and flanged RCSWs.

4.2 ACI 318 and NEHRP provisions for special structural walls to prevent local buckling.

Observed damage in recent earthquakes and laboratory studies of RCSWs and prisms replicated as boundary elements suggest that slim boundary regions can be prone to local inelastic buckling under cyclic load reversals. However, ACI 318 Chapter 21 does not provide limits on slenderness of special structural walls.

Considering this fact, the National Earthquake Hazards Reduction Program (NEHRP) (Moehle et al., 2012) recommended a ratio between the clear story height l_u and the wall thickness b no greater than 10, $l_u/b \leq 10$, within the length of the plastic hinge region and no greater than 16, $l_u/b \leq 16$, elsewhere. The second limit was prescribed in the 1997 Uniform Building Code.

Regarding the assessment of the NEHRP recommendation, no studies have been conducted.

4.3 Local buckling prediction assessment

Although different parameters have been explored as noticed in the previous sections, data still seem to be deficient and sometimes unconvincing when comparing proposed analytical solutions with actual behaviors observed in the field and laboratory. In this context, Herrick (2014) studied the differences between the Paulay and Priestley buckling model (PPBM) in comparison to Chai and Elayer buckling model (CEBM) when applied to walls tested in the past. Figure 8 represents the in-plane largest displacements before buckling occurred for the

walls included in Herrick's database when subjected to reversed cyclic loading. These experimental values were normalized to the displacements calculated from PPBM and CEBM associated with the maximum longitudinal tension strains sustained prior to buckling. A moment curvature sectional analysis program, CumbiaWall, was used for this purpose. Note that the prediction of the CEBM agrees better than the PPBM. It is important to mention that some walls from Herrick's database were not tested with the purpose of capturing inelastic buckling.

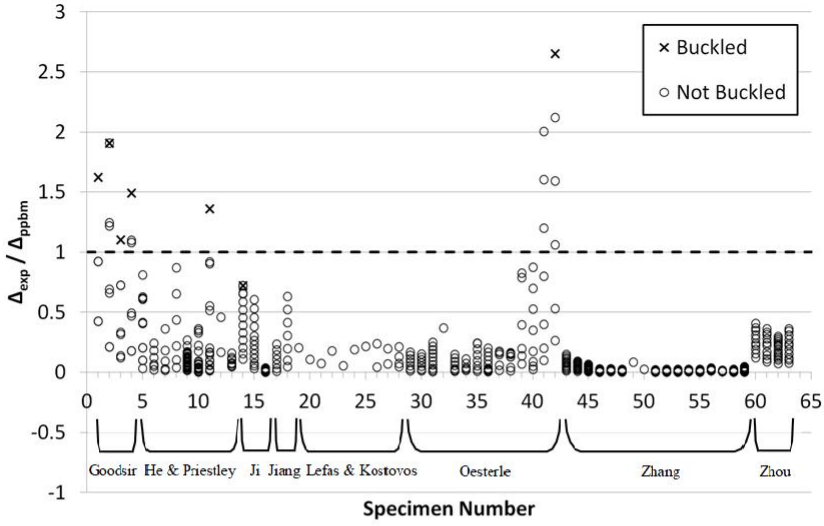

(a) Normalized to PPBM displacements

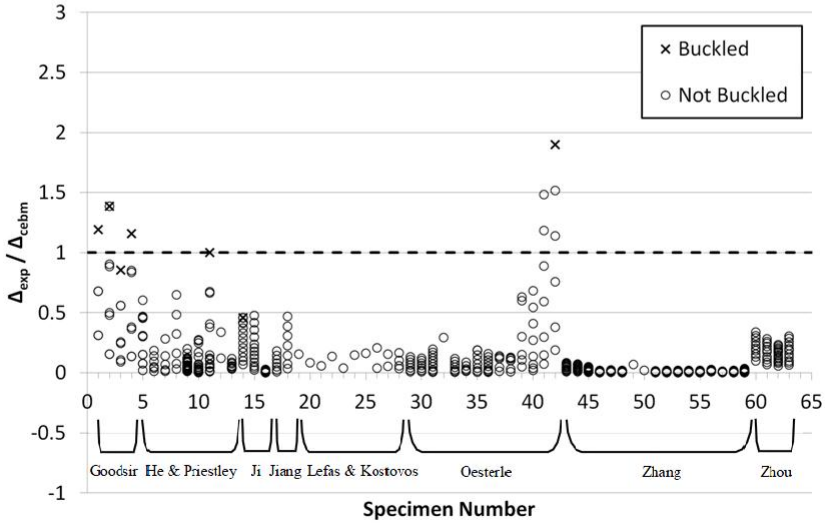

(b) Normalized to CEBM displacements

Figure 8 Wall experimental displacements normalized to PPBM and CEBM displacements. (Herrick, 2014)

A complimentary analysis was conducted in the same study. Considering the PPBM and CEBM models, Herrick (2014) established a failure limit state related to the sustainable buckling tensile strains for some of the prisms mentioned before in this document. Once the experimental tensile strains were identified for each case, they were compared with the predicted values demonstrating that the PPBM shows more discrepancy than the CCBM, which can be perceived from Figure 9.

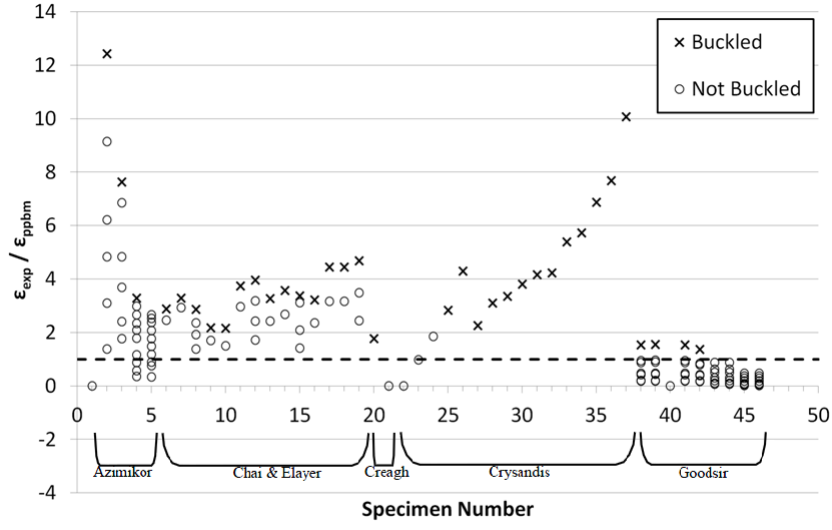

(a) Normalized to PPBM strains

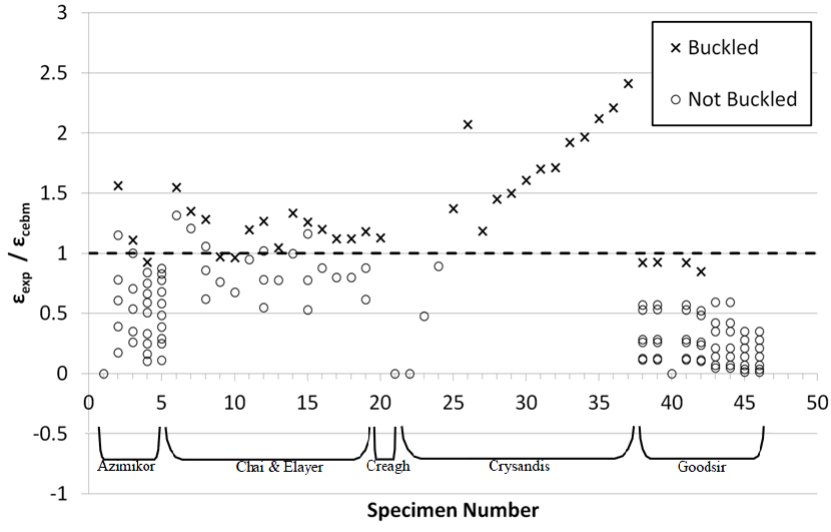

(b) Normalized to CEBM strains

Figure 9 Experimental prism strains normalized to PPBM and CEBM strains. (Herrick, 2014)

Note that monotonic loading cases were set as “zero” in both examinations, for walls and prisms. The symbol ‘x’ represents cycles where buckling instability was detected, and ‘o’ denotes the cycles where buckling was not captured. The specimens were assumed to suffer a buckling failure mode after detecting significant loss of strength, in the range between 10% and 30%, accompanied by a visible out-of-plane displacement.

As described by Herrick (2014), the two models are promising at predicting out-of-plane buckling of prisms; however, when applied to walls, the predictions tend to be conservative and they separate from the actual values exhibited in some tests.

5 FUTURE WORK

Additional investigations are suggested to detect the effect of missing parameters and the actual influence of established variables considered to be significant for stability.

Laboratory tests and field observations produce treasured data with significant outcomes that can be incorporated in seismic design guidelines. It is essential to be aware of the limitations of different methods in order to valid the predictions against experimental data.

6 CONCLUSIONS AND REMARKS

Based on the observed damage in the 27 February 2010 and the 22 February 2011 earthquakes, and the structural performance of RCSWs observed in experimental programs, updates to codes and guides are required to design and assess planar special RCSWs to prevent an inelastic instability associated with out-of-plane buckling. Recommendations such as minimum wall thickness for given seismic demands entail further research.

The tensile strains reached in the boundary elements of RCSWs during cyclic load reversals are critical and need to be limited. The influence of additional parameters like longitudinal and transverse reinforcement distributions, geometry aspect ratios, axial load ratios considered in the boundary elements calls for more in-depth studies.

The basics of two phenomenological models and a guideline to prevent out-of-plane buckling in RCSWs were described. Even though these recommendations suggest more analysis, they represent promising tools.

7 ACKNOWLEDGEMENTS

The research described in this paper is partially supported by the Instituto Ecuatoriano de Crédito Educativo y Becas (IECE); the Secretaría de Educación Superior Ciencia y Tecnología e Innovación, Ecuador; and the Universidad de las Fuerzas Armadas ESPE, Ecuador. This study form part of the PhD studies conducted at the North Carolina State University, Raleigh, under the direction of Dr. M. Kowlasky.

Any opinions, findings and conclusions articulated in the paper are those of the author and do necessarily reflect the view of the sponsors, organizations or other individuals mentioned here.

8 REFERENCES

1. Aaleti, S., Brueggen, B. L., Johnson, B., French, C. E., & Sritharan, S. (2013). Cyclic Response of RC Walls with Different Anchorage Details: An Experimental Investigation. *Journal of Structural Engineering*, (July).
2. Alarcón, M. (2013). *Influence of Axial Load in the Seismic Behavior of Reinforced Concrete Walls with Nonseismic Detailing.* Santiago de Chile: Pontificia Universidad Católica de Chile.
3. Berg, G., Bolt, B., Sozen, M., & Rojahn, C. (1980). *Earthquake in Romania March 4, 1977: An Engineering Report.* Washington: National Avademy Press.
4. Birely, A. (2011). *Seismic Performance of Slender Reinforced Concrete Structural Walls.* Washington: University of Washington.
5. Bostenaru, M., & Sandu, I. (2 de July de 2003). *Earthquake Engineering Research Institute.* World Housing Encyclopedia Report. https://www.eeri.org/lfe/pdf/romania_reinforced_concrete_cast.pdf
6. Brueggen, B. L. (2009). *Performance of T-shaped Reinforced Concrete Structural Walls under Multi-Directional Loading.* Minneapolis: University of Minnesota.
7. CESMD. (2014). *San Fernando Earthquake of 09 Feb 1971*. Obtenido de CESMD Internet Data Report: http://strongmotioncenter.org/cgi-bin/CESMD/
8. Chai, Y. H., & Elayer, D. T. (1999). Lateral Stability of Reinforced Concrete Columns under Axial Reversed Cyclic Tension and Compression. *ACI Structural Journal*, 780-789.

9. Christensen, D. (2002). *The Great Alaska Earthquake of 1964* . Obtenido de Alaska Earthquake Information Center: http://www.aeic.alaska.edu/Seis/quakes/Alaska_1964_earthquake.html

10. Chrysanidis, T. A., & Tegos, I. A. (2012). The influence of ratio of the longitudinal reinforcement of the boundary edges of structural walls to the resistance against lateral instability of earthquake-resistant reinforced concrete structural walls. *15 WCEE.* Lisboa.

11. Chrysanidis, T. A., & Tegos, I. A. (2012). The influence of tension strain of wall ends to their resistance against lateral instability for low-reinforced concrete walls. *15 WCEE.* Lisboa.

12. Considère, A. (September de 1891). Résistance des pièces comprimées. *Congrès International des Procédés de Construction. 3*, pág. 371. Paris: Librairie Polytechnique.

13. EEFIT. (1986). *The Mexican Earthquake of 19th September 1985.* London: Ove Arup and Partners.

14. EEFIT. (1993). *The Loma Prieta Earthquake of 17 October 1989 .* London: EEFIT.

15. EEFIT. (1994). *The Northridge, California Earthquake of 17 January 1994.* London: EEFIT.

16. EEFIT. (2003). *The Kocaeli, Turkey Earthquake of 17 August 1999 .* London: EEFIT.

17. EERL. (1971). *Engineering Features of the San Fernando Earthquake of February 9, 1971.* Pasadena, California: National Science Foundation, Earthquake Research Affiliates of the California Institute of Technology.

18. ESEE. (1995). *Selected Engineering Seismology and Structural Engineering Studies of the Hyogo-ken Nanbu (Great Hanshin) Earthquake of 17 January 1995.* London: ESEE .

19. Fattal, G., Simiu, E., & Culver, C. (1977). *Observations on the Behavior of Buildings in the Romania Earthquake of March 4, 1977.* Washington: U.S Department of Commerce. National Bureau of Standars.

20. Flintrop, A. (6 de September de 2013). *Testing of Reinforced Concrete Shear Wall Boundary Elements Designed According to ACI 318-11.* Obtenido de NEES: nees.org

21. GEM-ECD. (s.f.). *Vrancea Romania 1977 (CAR)*. Obtenido de Global Earthquake Model: http://gemecd.org/event/170

22. Goodsir, W. J. (1985). *The Design of Coupled Frame-Wall Structures for Seismic Actions.* Christchurch, New Zealand: University of Canterbury.

23. Hansen, W. (1965). *Effects of the Earthquake of March 27, 1964, at Anchorage, Alaska.* Washington: United States Government Printing Office .

24. Herrick, K. (2014). *An Analysis of Local Out-of-Plane Buckling of Ductile Reinforced Structural Walls Due to In-Plane Loading.* Raleigh: North Carolina State University.

25. Jasinski, F. (22 de June de 1895). Noch ein Wort zu den 'Knickfragen,'. *Schweizerische Bauzeitung, 25*, 172-175.

26. Jünemann, R., Hube, M., & De La Llera, J. (2012). Characteristics of Reinforced Concrete Shear Wall Buildings Damaged During 2010 Chile Earthquake. *15 WCEE.* Lisboa: WCEE.

27. Kam, W., Pampanin, S., & Elwood, K. (December de 2011). Seismic Performance of Reinforced Concrete Buildings in the 22 February Christchurch (Lyttelton) Earthquake. *Bulletin of the New Zealand Society for Earthquake Engineering, 44, No. 4*, págs. 239-278.

28. MAE Center. (2010). *The Maule (Chile) Earthquake of February 27, 2010. Consequence Assessment and Case Studies.* Urbana-Champaign: MAE Center.

29. Marihuén, A. N. (2014). *Comportamiento Sísmico de Muros Esbeltos de Hormigón Armado.* Santiago de Chile, Chile: Pontificia Universidad Católica de Chile.

30. Moehle, J. P., Hooper, J. D., Fields, D. C., & Gedhada, R. (2012). Seismic Design of Cast-in-Place Concrete Special Structural Walls and Coupling Beams A Guide for Practicing Engineers. *NEHRP Seismic Design Technical Brief*, (6).

31. Moroni, O. (2002). *World Housing Encyclopedia.* Obtenido de http://www.world-housing.net/: http://www.world-housing.net/wp-content/uploads/2011/08/Type_RC_Wall.pdf

32. National Research Council (U.S.). Committee on the Alaska Earthquake. (1973). *The Great Alaska Earthquake of 1964. Engineering.* Washington. D.C.: National Academy of Sciencie .

33. Oesterle, R. G., Fiorato, a. E., Johal, L. S., Carpenter, J. E., Russell, H. G., & Corley, W. G. (1976). Earthquake resistant structural walls - Tests of isolated walls.

34. Oesterle, R. G., Fiorato, A. E., Aristizabal-Ochoa, J. D., & Corley, W. G. (1979). Earthquake Resistant Structural Walls - Tests of Isolated Walls. 243-273.

35. Paulay , T., & Priestley, M. (1993). Stability of Ductile Structural Walls. *ACI Structural Journal, Vol. 90, No. 4*, 385-392.

36. Paulay, T., & Goodsir, W. (1985). The Ductility of Structural Walls. *Bulletin on the New Zealand National Society for Earthquake Engineering, 18*, 250-269.

37. Paulay, T., & Priestley, M. (1992). *Seismic Design of Reinforced Concrete and Masonry Buildings.* New York: John Wiley and Sons.

38. PEER. (2000). *Structural Engineering Reconnaissance of the August 17, 1999 Earthquake: Kocaeli (Izmit), Turkey.* Berkeley: PEER.

39. Rutenberg, A., Jennings, P., & Housner, G. (1980). *The Response of Veterans Hospital Building 41 in the San Fernando Earthquake.* Pasadena, California: Earthquake Engineering Research Laboratory.

40. SCEDC. (2013). *Significant Earthquakes and Faults. San Fernando Earthquake* . Obtenido de Southern California Earthquake Data Center : http://www.data.scec.org/significant/sanfernando1971.html

41. Saatcioglu, M., Palermo, D., Ghobarah, A., Mitchell, D., Simpson, R., Adebar, P., … Hong, H. (2013). Performance of reinforced concrete buildings during the 27 February 2010 Maule (Chile) earthquake1. *Canadian Journal of Civil Engineering*, *40*(July), 693–710.

42. Shea, M. (6 de September de 2013). *Seismic Peformance of Thin Reinforced Concrete Shear Wall Boundaries.* Obtenido de NEES: nees.org

43. Sritharan, S. (2011). The M6.3 Christchurch Earthquake: Performance of Buildings in CBD. *Quake Summit 2011.* Buffalo, New York: EERI.

44. Sritharan, S., Beyer, K., Henry, R. S., Chai, Y. H., Kowalsky, M., & Bull, D. (2014). Understanding Poor Seismic Performance of Concrete Walls and Design Implications. *Earthquake Spectra, Vol. 30, No. 1*, 307-334.

45. Su, N. (2001). Structural Evaluation of Reinforced Concrete Buildings Damaged by Chi-Chi Earthquake in Taiwan. *Practice Periodical on Structural Design and Construction*, 119-128.

46. Thiel, K., Wenk, T., & Bachmann, H. (2000). *Versuche an Stahlbetontragwänden unter pseudodynamischer Einwirkung.* Zürich: Institut für Baustatik und Konstruktion.

47. Thomsen, J. H., & Wallace, J. W. (2004). Displacement-Based Design of Slender Reinforced Concrete Structural Walls—Experimental Verification. *Journal of Structural Engineering*, 618-630.

48. U.S. Geological Survey. (1985). *Preliminary Report of Investigations of the Central Chile Earthquake of March 3, 1985* . Denver, Colorado: Department of the Interior - U.S. Geological Survey.

49. USGS. (2014). *The Great Alaska Earthquake and Tsunami of March 27, 1964*. Obtenido de USGS Science for a Changing World: http://earthquake.usgs.gov/earthquakes/events/alaska1964/

50. Vallenas, J., Bertero, V., & Popov, E. (1979). *Hysteretic Behavior of Reinforced Concrete Structural Walls.* Berkeley, California: Earthquake Engineering Research Center.

51. W.Y., K., & Pampanin, S. (2011). The seismic performance of RC buildings in the 22 February 2011 Christchurch earthquake. *Structural Concrete*, 223-233.

52. Wallace, J. W. (2012). Behavior, Design, and Modeling of Structural Walls and Coupling Beams - Lessons from Recent Laboratory Tests and Earthquakes. *International Journal of Concrete Structures and Materials, Vol. 6, No. 1*, 3-18.

53. Wallace, J. W., & Moehle, J. (2012). Behavior and Design of Structural Walls – Lessons from Recent Laboratory Tests & Earthquakes. *International Symposium on Engineering Lessons Learned from the 2011 Great East Japan Earthquake*, (págs. 1132-1144). Tokyo, Japan.

54. *Wikipedia, the free encyclopedia*. (30 de May de 2014). Obtenido de 2010 Chile Earthquake: http://en.wikipedia.org/wiki/2010_Chile_earthquake